

See discussions, stats, and author profiles for this publication at: <https://www.researchgate.net/publication/6541666>

Dynamic Kinetic Capillary Isoelectric Focusing: A Powerful Tool for Studying Protein–DNA Interactions

ARTICLE *in* ANALYTICAL CHEMISTRY · MARCH 2007

Impact Factor: 5.64 · DOI: 10.1021/ac061876c · Source: PubMed

CITATIONS

23

READS

42

4 AUTHORS, INCLUDING:



Andrei P Drabovich

University of Toronto, University Health Net...

36 PUBLICATIONS 978 CITATIONS

SEE PROFILE



Sergey N Krylov

York University

167 PUBLICATIONS 3,625 CITATIONS

SEE PROFILE



Janusz Pawliszyn

University of Waterloo

516 PUBLICATIONS 25,077 CITATIONS

SEE PROFILE

Dynamic Kinetic Capillary Isoelectric Focusing: A Powerful Tool for Studying Protein–DNA Interactions

Zhen Liu,^{*,†} Andrei P. Drabovich,[‡] Sergey N. Krylov,[‡] and Janusz Pawliszyn[§]

Department of Chemistry, Nanjing University, Nanjing 210093, China, Department of Chemistry, York University, Toronto, Ontario M3J 1P3, Canada, and Department of Chemistry, University of Waterloo, Waterloo, Ontario N2L 3G1, Canada

A new method called dynamic kinetic capillary isoelectric focusing (DK-CIEF) is presented for the study of protein–DNA interactions. The method is based on CIEF with laser-induced fluorescence-whole column imaging detection in which protein–DNA complexes are separated with spatial resolution while dissociations of the complexes are dynamically monitored using a CCD camera with temporal resolution. This method allows for the discrimination of different complexes and the measurement of the individual dissociation rate constants.

Protein–DNA interactions play important roles in many biological processes, including gene expression, DNA replication, DNA integrity control, and DNA damage repair. To improve our understanding of these biological processes, it is important to understand both the kinetics and the mechanism of protein–DNA interactions. Usually, the formation and dissociation of a protein–DNA complex (PD) can be described as below,



where P and D are free protein and free DNA, respectively, k_{on} is the association rate constant, and k_{off} is the dissociation rate constant of the complex. The stability of the protein–DNA complex can be described in terms of the dissociation constant, $K_d = k_{\text{off}}/k_{\text{on}}$, or binding constant, $K_b = 1/K_d$.

To date, electrophoresis has been the workhorse method for in vitro studies of protein–DNA interactions. Classical electrophoresis mobility shift assay (EMSA)¹ and its new variant, capillary electrophoresis (CE)-based mobility shift assay (CEMSA),^{2,3} have been widely used for the measurement of binding constants. However, the assumption of equilibrium in these methods makes it difficult or impossible to determine the kinetic parameters. Until recently, the only method with comprehensive kinetic capabilities was surface plasmon resonance (SPR).⁴ However, because the SPR

approach requires that one of the interacting species be immobilized onto a solid substrate, this method often suffers from nonspecific binding to the surface and changes in the binding constant.

More recently, a general conceptual kinetic analysis platform, referred to as kinetic capillary electrophoresis (KCE), has been proposed.⁵ KCE is defined as the CE separation of species that interact during electrophoresis. Different KCE methods can be designed by arranging different initial and boundary conditions for the interactions. In addition to two previously reported kinetic methods, nonequilibrium capillary electrophoresis of equilibrium mixtures (NECEEM)^{6–9} and sweeping capillary electrophoresis (sweepCE),¹⁰ four new methods have been designed according to this generic concept. These KCE methods exhibit different strengths for kinetic analysis. For example, NECEEM offers a more accurate measurement of k_{off} than k_{on} whereas sweepCE is more sensitive to k_{on} than k_{off} . Based on the six well-defined methods, a multimethod KCE toolbox was proposed as an integrated kinetic technique.⁵ With use of the KCE toolbox, measurements of individual kinetic parameters for different interactions became possible.

The current KCE methods are mainly based on the capillary zone electrophoresis (CZE) mode; the electropherogram for the kinetic analysis is the profile of the signal vs time. When different protein–DNA complexes are formed, the presentation of the separation of these complexes is still the same signal vs time profile; in other words, the resolution for different complexes in these methods is parallel to the resolution for difference in the kinetic parameters. The parallel resolutions lead to invalidation of “easy-math” based KCE methods such as NECEEM (vide infra). One solution is to use other KCE methods such as short SweepCE (sSweepCE); however, such methods rely on more involved mathematics (nonlinear regression analysis) to deconvolute the overlapped signal.

(4) Wilson, W. D. *Science* **2002**, *295*, 2103–2105.

(5) Petrov, A.; Okhonin, V.; Berezovski, M.; Krylov, S. N. *J. Am. Chem. Soc.* **2005**, *127*, 17104–17110.

(6) Berezovski, M.; Krylov, S. N. *J. Am. Chem. Soc.* **2002**, *124*, 13674–13675.

(7) Krylov, S. N.; Berezovski, M. *Analyst* **2003**, *128*, 571–575.

(8) Okhonin, V.; Krylova, S. M.; Krylov, S. N. *Anal. Chem.* **2004**, *76*, 1507–1512.

(9) Krylova, S. M.; Musheev, M.; Nutiu, R.; Li, Y.; Lee, G.; Krylov, S. N. *FEBS Lett.* **2005**, *579*, 1371–1375.

(10) Okhonin, V.; Berezovski, M.; Krylov, S. N. *J. Am. Chem. Soc.* **2004**, *126*, 7166–7167.

* To whom correspondence should be addressed. E-mail: zhenliu@nju.edu.cn.

[†] Nanjing University.

[‡] York University.

[§] University of Waterloo.

(1) Laniel, M.-A.; Beliveau, A.; Guerin, S. L. *Methods Mol. Biol.* **2001**, *148*, 13–30.

(2) Foulds, G. J.; Etzkorn, F. A. *Nucleic Acids Res.* **1998**, *26*, 4304–4305.

(3) Wan, Q.-H.; Le, C. *Anal. Chem.* **2000**, *72*, 5583–5589.

To overcome these limitations, we propose a new kinetic analysis method called dynamic kinetic capillary isoelectric focusing (DK-CIEF) by introducing a new type of resolution into the KCE concept. CIEF is a high-resolution CE mode for the separation of amphoteric biomolecules, particularly proteins, according to differences in the isoelectric point (pI). CIEF with whole column imaging detection (WCID)^{11–16} is a novel CIEF format in which proteins are focused into stationary bands in a pH gradient within a short capillary under the influence of an electric field and the focused protein bands in the whole column are dynamically detected using a CCD camera. The resolution of different proteins is expressed using a profile of signal vs position in a pH gradient. Moreover, the dynamic detection capability of the WCID allows for real-time monitoring of the change in peak areas of the complexes. The copresence of the spatial and temporal resolution in the CIEF-WCID makes it a very capable tool for kinetic analysis. When a mixture of an interacting pair of protein and DNA is introduced into the CIEF-WCID system for focusing, the free protein and the protein–DNA complexes are focused into stationary bands while the free DNA (including the initially unbound portion and the portion released from the complexes due to dissociation) are electrokinetically pumped out of the separation column under the applied electric field. With application of a fluorescently labeled DNA, the peak areas for the complexes will gradually decrease due to the dissociation, and the selective laser-induced fluorescence (LIF) detection of the protein–DNA complexes avoids possible interference from the focused protein band. Thus, the mechanism and kinetics of the interactions can be deciphered and determined according to the signal vs position profile and the dependence of peak area vs dissociation time. In this study, we use an *E. coli* single-stranded DNA binding protein (SSB) and a fluorescently labeled 15-mer oligonucleotide (fDNA) as an interacting model to demonstrate the powerful kinetic capability of the proposed DK-CIEF approach.

EXPERIMENTAL SECTION

Instrumentation. The DK-CIEF experiments were carried out on an in-house built CIEF–LIF–WCID system described previously.^{12,13} The separation column was 150 μm i.d. \times 350 μm o.d. \times 5 cm Teflon AF 2400 capillary (Random Technologies, San Diego, CA). The excitation wavelength was 488 nm produced by an air-cooled argon ion laser. Emitted light was filtered by a long-pass filter (530 nm cutoff) prior to detection. The NECEEM experiments were carried out on a P/ACE MDQ system (Beckman Coulter, Fullerton, CA) equipped with a LIF detector. The 488 nm line of an argon ion laser was used to excite fluorescence. An uncoated fused-silica capillary 48.6 cm (38.5 cm to the detection window) in length with 75 μm i.d. and 360 μm o.d. was used. The temperature of the capillary was maintained at 20 ± 0.1 °C.

Chemicals. The SSB (15.87 μM in concentration), pharmalytes (pH 3–10, 40% in concentration), poly(vinylpyrrolidone) (PVP, average molecular weight about 360000, and intrinsic viscosity 80–100 K), and cytochrome C were purchased from Sigma (St.

Louis, MO). The 5'-6-carboxyfluorescein-GCGGAGCGTGGCAGG (fDNA, 10 μM in concentration) was from Integrated DNA Technologies (Coralville, IA). NanoOrange kit was from Molecular Probes (Eugene, OR). The anolyte and catholyte were 100 mM phosphoric acid and 100 mM sodium hydroxide, respectively. Water (18 M Ω) was purified with an ultrapure water system (Barnstead/Thermolyne, Dubuque, IA).

Sample Preparation. For DK-CIEF experiments of SSB–fDNA, 0.5 μL of SSB and 1 μL of fDNA were mixed with 10 μL of borate buffer (200 mM, pH 9.3) and then incubated at room temperature for 15 min, protected from light. Subsequently, the mixture was mixed with 5 μL of pharmalytes (pH 3–10), 5 μL of poly(vinylpyrrolidone) (10% w/v), and 78.5 μL of water. For the experiments of cytochrome C–NanoOrange complex, 10 μL of cytochrome C (1 mg/mL) and 100 μL of 1X NanoOrange working solution were mixed and incubated under room temperature for 60 min, protected from light. The mixture was mixed with 50 μL of pharmalytes (pH 3–10), 50 μL of PVP (10% w/v), and 790 μL of water. For NECEEM of SSB–fDNA, certain amounts of SSB and fDNA were mixed and dissolved in 50 mM Tris-acetate (pH 8.2) and then incubated at room temperature for 15 min, protected from light, giving a final concentration of 150 nM fDNA and 200 nM SSB.

DK-CIEF. The prepared sample was injected to fill the whole separation column. A 500 V potential was used to initiate the focusing and the voltage was increased to 3 kV at 5 min. The LIF signal was monitored with the desired interval from 12 min, when the complexes had been well-focused.

NECEEM. The inlet and outlet reservoirs contained the run buffer (50 mM Tris-acetate, pH 8.2), and the capillary was prefilled with the run buffer. A plug of the SSB–DNA equilibrium mixture was injected into the capillary by a pressure pulse of 5 s \times 0.5 psi. An electric voltage of 25 kV was applied to run electrophoresis.

RESULTS AND DISCUSSION

Carrier Ampholytes (CAs) Interference. In this study, we assume that the presence of CAs does not disturb protein–DNA binding. If such an assumption is not true, there are two possibilities that interfere with the binding: (1) CAs–protein interaction and (2) CAs–DNA interaction. Using CIEF–WCID, we can investigate if such interactions occur. The SSB and fDNA were mixed with CAs, respectively, and then DK-CIEF experiments were carried out. If there is any CAs–SSB or CAs–fDNA complex formed, it will be detectable in the focusing process. As the SSB lacks fluorophore, the focusing process was monitored with UV absorbance–WCID at 280 nm. However, there were no other peaks, except for one peak at pI = 6.0 (the measured pI value is in good agreement with the literature value for the SSB). The possibility of CAs–fDNA interaction was excluded with CIEF–LIF–WCID experiments since no peak was observed within the whole column.

Photobleaching. Photobleaching is another issue that needs to be considered because it may influence the measurement accuracy and even make measurement impossible. Our previous results indicated that when the exposure time is short enough (≤ 250 ms), fluorescence signal loss due to laser shot is very slight. Experiment was not carried out to investigate the photobleaching of fDNA in this study, as fDNA cannot be focused in CIEF. We assume the influence of photobleaching is ignorable. To reduce

(11) Wu, J.; Watson, A. H.; Torres, A. R. *Am. Biotechnol. Lab.* **1999**, 17, 24–26.

(12) Liu, Z.; Pawliszyn, J. *Anal. Chem.* **2003**, 75, 4887–4894.

(13) Liu, Z.; Pawliszyn, J. *Anal. Biochem.* **2005**, 336, 94–101.

(14) Liu, Z.; Pawliszyn, J. *J. Proteome Res.* **2004**, 3, 567–571.

(15) Liu, Z.; Pawliszyn, J. *Anal. Chem.* **2005**, 77, 165–171.

(16) Liu, Z.; Lemma, T.; Pawliszyn, J. *J. Proteome Res.* **2006**, 5, 1246–1251.

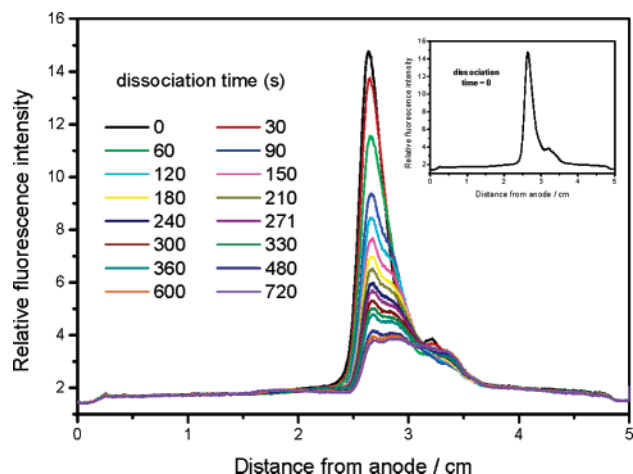


Figure 1. CIEF profiles of the SSB–fDNA complexes at consecutive dissociation times. The insertion highlights the CIEF profile at dissociation time equal to zero.

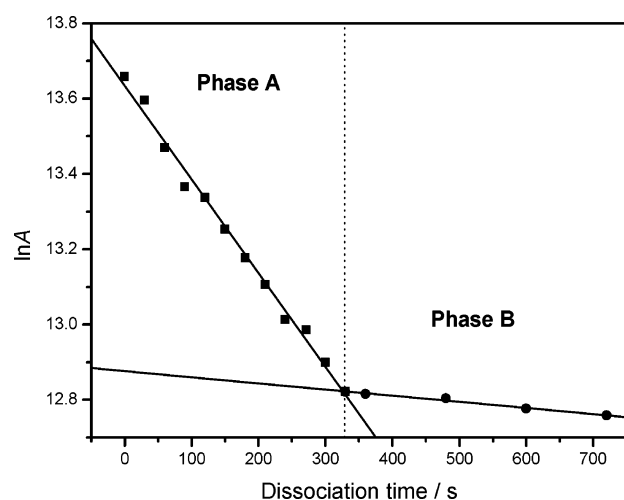


Figure 2. Dependence of the natural logarithm of the total peak area of the SSB–fDNA complexes on the dissociation time. Two dissociation phases were involved: phase A (square) and phase B (dot).

the influence of photobleaching on the measurement accuracy particularly for slow dissociation, the interval between two consecutive images was extended long enough.

DK-CIEF of SSD–fDNA. Figure 1 illustrates the CIEF profiles of the SSB–fDNA complexes at consecutive dissociation times. When the dissociation time equals zero, two overlapped peaks were observed. The presence of the two peaks indicates the formation of two SSB–fDNA complexes. The minor peak exhibited a higher pI than the major peak. The peak area decreased as the decay time increased. Because the dissociation of the SSB–fDNA complexes obeys a first-order reaction model, the dependence of the natural logarithm of the peak area ($\ln A$) on the dissociation time (t_d) for an individual complex should follow a linear relationship. Because of the peak overlapping, the total peak area was measured for the two peaks. The natural logarithm of the total peak area ($\ln A$) was plotted against t_d , as shown in Figure 2. It is apparent that the $(\ln A) - t_d$ plot can be divided into two linear relationships, indicating the presence of two dissociation phases: one with a relatively abrupt slope (phase A) and one with a relatively flat slope (phase B). The $(\ln A) - t_d$

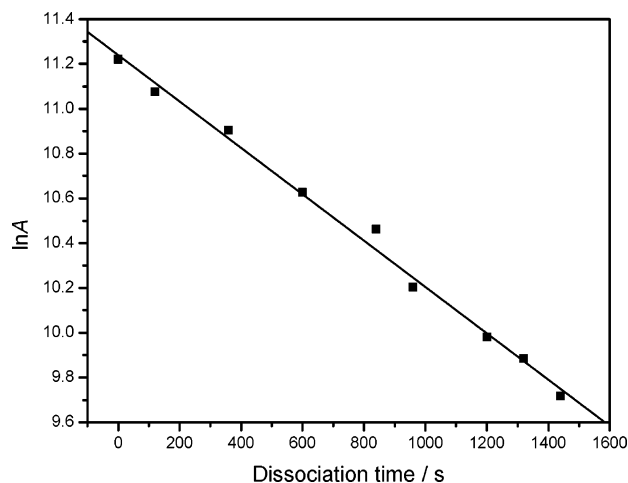


Figure 3. Dependence of the natural logarithm of the peak area of nonspecific cytochrome C–NanoOrange complex on the dissociation time observed by CIEF–LIF–WCID.

dependence for both phase A and phase B exhibited good linearity, with a correlation coefficient of greater than 0.99. Moreover, the slopes of the linear relationships were repeatable; for instance, the slopes for phase A were measured to be -2.58 , -2.53 , and $-2.49 \times 10^{-3} \text{ s}^{-1}$ for three consecutive runs. It can be seen that the dissociation in phase A is due to the sum of the dissociations of the low-pI complex and the high-pI complex while the dissociation in phase B is only due to the dissociation of the high-pI complex. Therefore, the k_{off} value for the high-pI complex is equal to the opposite value of the slope for phase B ($1.83(\pm 0.19) \times 10^{-4} \text{ s}^{-1}$) whereas the k_{off} value for the low-pI complex equals the opposite value of the difference between the slopes for phase A and the slope for B ($2.35(\pm 0.24) \times 10^{-3} \text{ s}^{-1}$).

Two types of interactions have previously been hypothesized for SSB and ssDNA: high-affinity specific binding and low-affinity nonspecific binding.^{17,18} The KCE toolbox has been applied to differentiate these types of interactions and it was found that nonspecific binding has a faster k_{off} than specific binding.⁵ For example, for a fluorescently labeled 40-mer ssDNA, the k_{off} was $8 \times 10^{-2} \text{ s}^{-1}$ and $6 \times 10^{-4} \text{ s}^{-1}$ for nonspecific and specific binding, respectively. The significantly different k_{off} values measured in this study suggest that the high-pI complex is representative of specific binding while the low-pI complex is representative of nonspecific binding.

DK-CIEF of Cytochrome C–NanoOrange. To confirm if the different dissociation rates of the SSB–fDNA complexes are due to different types of interactions, we investigated the binding of cytochrome C and NanoOrange. NanoOrange is a noncovalent fluorescent dye and can bind to proteins through hydrophobic and electrostatic interactions (nonspecific). Like the fDNA, NanoOrange is also negatively charged under the experimental conditions used and thus unbound NanoOrange will be pumped out of the separation column under the electric field. As shown in Figure 3, the $(\ln A) - t_d$ plot for cytochrome C–NanoOrange complex obeyed a single linear relationship, completely different

(17) Ferrai, M. E.; Bujalowski, W.; Lohman, T. M. *J. Mol. Biol.* **1994**, *236*, 106–123.

(18) Hagmar, P.; Dahlman, K.; Takahashi, M.; Carstedt-Duke, J.; Gustafsson, J.; Norden, B. *FEBS Lett.* **1989**, *253*, 28–32.

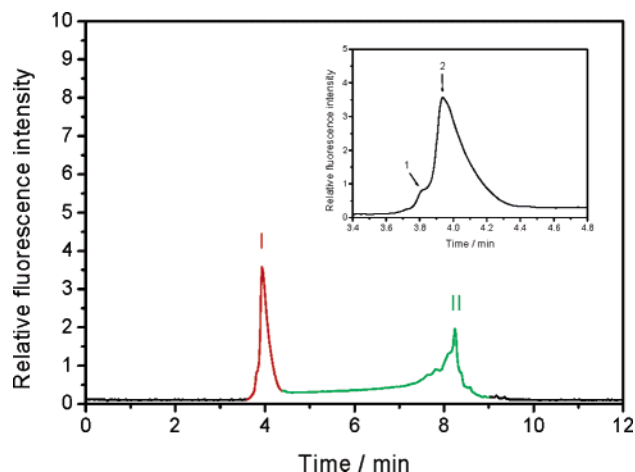


Figure 4. NECEEM electropherogram of the SSB-fDNA complexes. The insertion is the zoom-in profile of peak I.

than that of the SSB-fDNA complexes. The dissociation rate constant was measured to be $1.04 \times 10^{-3} \text{ s}^{-1}$. The single dissociation behavior observed for the nonspecific NanoOrange-cytochrome C binding suggests that the SSB-fDNA interactions involved both nonspecific and specific binding.

NECEEM. NECEEM experiments were performed for the SSB-fDNA interacting system for comparison. A representative NECEEM electropherogram is shown in Figure 4. Peak I (red) represents the SSB-fDNA complexes while peak II (blue) denotes fDNA molecules released from the complexes. A close-up view of peak I discloses that it is composed of two overlapped peaks (see the insertion of Figure 4), indicating the presence of two different SSB-fDNA complexes. Because of the peak overlapping, however, the NECEEM approach failed to determine individual dissociation rate constants for each protein-DNA complex formed. Without considering the difference between the two complexes, an apparent k_{off} value of $2.09(\pm 0.07) \times 10^{-3} \text{ s}^{-1}$ was found according to the calculation method reported previously.⁷ Clearly, compared with NECEEM, the DK-CIEF approach is advantageous; it permits not only the discrimination of different types of interactions but also the measurement of individual dissociation rate constants.

Specific Binding vs Nonspecific Binding. Based on the above results and discussion, it can be seen that the high-pI complex was the product due to specific binding whereas the low-pI complex was formed by nonspecific binding. The k_{off} value for specific and nonspecific binding is $1.83(\pm 0.19) \times 10^{-4}$ and $2.35(\pm 0.24) \times 10^{-3} \text{ s}^{-1}$, respectively. The slight pI difference between the SSB-fDNA complexes formed by specific and nonspecific binding may suggest that different binding sites are involved so that the changes in the surface charge of the protein are different.

CONCLUSIONS

A dynamic kinetic approach has been developed for the study of protein-DNA interactions. The CIEF-WCID technique contributes to the dynamic kinetic capability of the approach; the spatial resolution permits the separation of the different complexes, and the temporal resolution allows for the measurement of the dissociation rate constant. Compared with individual current KCE methods, the proposed method offers a significant advantage: it allows for the discrimination of different types of interactions and the measurement of individual dissociation rate constants. Compared with the KCE integrated toolbox, which relies on nonlinear regression analysis, this method provides another significant advantage: it requires only "easy-math". It should be noted that the approach proposed can measure only the dissociation rate constant at the present stage. To obtain complete kinetic information, a set of experiments at a series of protein and DNA concentrations should be involved, which allows for direct measurement of the binding constant and indirect measurement of the association rate constant.

ACKNOWLEDGMENT

We thank Dr. Maxim Berezovski for his useful discussions. Z.L. acknowledges National Natural Science Foundation of China for financial support (Grant No. 20521503).

Received for review October 6, 2006. Revised. Accepted November 17, 2006.

AC061876C